Influence of FeO and H on the electrical conductivity of olivine

Lidong Dai [a,b], Shun-ichiro Karato [b,*]

[a] Key Laboratory for High Temperature and High Pressure Study of the Earth's Interior, Institute of Geochemistry, Chinese Academy of Sciences, Guiyang, Guizhou 550002, China
[b] Department of Geology and Geophysics, Yale University, New Haven, CT 06511, USA

ABSTRACT

The influence of Fe (iron) and H (hydrogen) on the electrical conductivity of olivine was investigated. Synthetic olivine aggregates with the X_{Fe} = Fe/(Fe + Mg) (molar ratio) = 21–64% with the water content of 84–620 ppm wt (Paterson calibration) were prepared and their electrical conductivity was measured at P = 4 GPa and T = 873–1473 K. The impedance spectroscopy was used to calculate the DC electrical conductivity. We found that electrical conductivity of samples increases with increasing FeO content in both anhydrous and hydrous olivine. However, the way in which FeO enhances electrical conductivity is different between anhydrous and hydrous olivine. In anhydrous sample, the activation energy is reduced with FeO content and hence the effect of FeO content is large at low temperatures, but its effect is small at mantle temperatures. In contrast, FeO content does not affect the activation energy in hydrous olivine, and consequently, the magnitude of FeO effect is nearly independent of temperature. For both anhydrous and hydrous olivine, the influence of FeO is only modest at high temperatures (increase in conductivity by a factor of $\sim$2 for the increase in FeO by 20% (e.g., from 10 to 30%)). In contrast, the FeO content has relatively large effects at low temperatures for anhydrous olivine. However, the role of hydrogen is large at low temperatures and hydrogen mechanism dominates under most cases. Therefore the influence of FeO on electrical conductivity is small at all temperatures for a plausible range of water content. We conclude that the water (hydrogen) content in a terrestrial planet can be inferred from observed conductivity without substantial influence of FeO if the temperature is constrained. The present results provide a basis for the interpretation of electrical conductivity model of other planets with different FeO contents.

© 2014 Elsevier B.V. All rights reserved.

1. Introduction

Electrical conductivity in minerals is enhanced by the presence of iron (FeO) and hydrogen (H) (e.g., (Karato and Wang, 2013; Yoshino, 2010)). This is interpreted by the model where the electric charge is transported by the electron transfer between ferric and ferrous iron ("polaron" conduction) and/or by the diffusion of hydrogen (proton). There have been extensive experimental studies to investigate each effect separately. For instance, Cemič et al. (1980) and Omura et al. (1989) determined the influence of FeO content on the electrical conductivity of anhydrous olivine. For obvious reasons, Fe-assisted conduction depends strongly on FeO content. Wang et al. (2006), Yoshino et al. (2009) and Yoshino et al. (2006) determined the effects of hydrogen content on the electrical conductivity of olivine. Similar to Fe-assisted conduction, hydrogen-assisted conduction depends strongly on hydrogen content.

However, it has not been studied if the FeO content has any appreciable effects on hydrogen-assisted conduction. Most of studies on hydrogen-assisted conduction were on San Carlos olivine where X_{Fe} (molar ratio of Fe/(Fe + Mg)) $\sim$ 0.1. Consequently, it is difficult to evaluate the electrical conductivity-depth profile in a planet where FeO content is likely different from Earth. An important example is Mars that is likely to have FeO-rich mantle, X_{Fe} $\sim$ 0.25 (Bertka and Fei, 1997). The Moon is also likely to have a higher FeO content (X_{Fe} $\sim$ 0.17; (Khan et al., 2007)), and if a model by Elkins-Tanton and Grove (2011) is used X_{Fe} would be as high as $\sim$0.6 in the deep lunar mantle. Also, olivine in the crustal rocks (e.g., gabbro) has much higher FeO content than mantle olivine. In contrast, Mercury appears to have less FeO than Earth (e.g., (Nittler et al., 2011)). If FeO content affects the electrical conductivity of olivine for the same hydrogen content, then the inference of hydrogen content of a planet with different FeO content will require a correction. Vacher and Verhoeven (2007) attempted to parameterize the influence of FeO on electrical conductivity of olivine for planetary applications, but they did not include the influence of hydrogen. Because the influence of hydrogen dominates under most of planetary conditions (e.g., (Karato, 1990; Karato

* Corresponding author. Tel.: +1 203 432 3147; fax: +1 203 432 3134.
E-mail address: shun-ichiro.karato@yale.edu (S.-i. Karato).

and Wang, 2013)), it is important to investigate the influence of FeO in hydrogen-dominated electrical conductivity.

One may consider two different cases. First is a case, where the influence of FeO and H is independent and hence the FeO content does not affect the conductivity due to proton. This would be the case if the presence of FeO does not enhance the proton mobility. Secondly, and opposite is a case where FeO and H effects interact. The latter would be the case where the mobility of proton is sensitive to the FeO content. In either case, because the solubility of H in olivine increases with FeO content (Zhao et al., 2004), electrical conductivity of olivine at a given water fugacity will always increase with FeO content. However, distinguishing these two cases is critical if one wishes to infer hydrogen content from geophysically inferred electrical conductivity of a planet with different FeO content (e.g., (Grott et al., 2013; Karato, 2013a)).

In order to test the validity of above two alternative models, we have conducted a series of experiments where we determined the influence of FeO and H content in the electrical conductivity of olivine. This paper reports the results and presents a microscopic model to explain the results and discusses the possible implications for electrical conductivity in other planets.

2. Experimental procedure

2.1. Sample preparation and characterization

High-purity (99.9%) powders of MgO and Fe_2O_3 with different percentages (molar ratio: ~20%, ~40% and ~60%) were homogenously mixed in the agate mortar, and (Mg, Fe)O with different FeO content were synthesized in a furnace under the controlled oxygen fugacity. Annealing was made in a room pressure furnace at T (temperature) = 1673 K for 18 h and a mixture of $CO + CO_2$ was used to attain the oxygen fugacity close to the Ni—NiO buffer. (Mg,Fe)O were then ground into powders with the grain size less than 5 μm, and SiO_2 was added to make the (Mg + Fe)/Si ratio close to 2 (however, the amount of SiO_2 was chosen to be slightly in excess ((Mg + Fe)/Si = 1.94)) to assure that a sample's oxide activity is buffered by the excess pyroxene). A mixture of (Mg,Fe)O and SiO_2 was cold-pressed, and then annealed at T = 1573 K under the controlled oxygen fugacity close to the Ni—NiO buffer for 12 h. Lastly, the pellets of synthetic polycrystalline olivine were ground into powders and cold pressed into pellets, and vacuum-sintered at T = 1573 K for 3 h. The vacuum-sintered samples have porosity less than ~2%. The chemical compositions of sample are shown in Table 1. The water content is less than ~10 $H/10^6$ Si. We call this "dry" olivine. We made hydrothermal annealing experiments at P = 4 GPa and T = 1573 K for 3 h using a Ni—NiO

buffer to control the oxygen fugacity. The details of hydrothermal annealing experiments are described by Dai and Karato (2009). The FT-IR spectroscopy of hydrothermally treated samples showed homogeneously distributed hydrogen. The grain-size of the samples is 5–10 μm.

In order to determine the water content of the samples, the infrared spectra of samples were obtained at wavenumbers from 1000 to 4000 cm^{-1} both before and after each experiment. The measurements were made using a Fourier transform infrared spectroscopy (FT-IR) spectrometer (BIORAD, Varian 600 UMA). Doubly polished samples with a thickness 50–80 μm were prepared for the IR analysis. The IR absorption of samples was measured by unpolarized radiation with a mid-IR light source, a KBr beam splitter and an MCT detector with a 100×100 μm^2 aperture. 256 scans were accumulated for each sample. The infrared spectra of the acquired for a sample with X_{Fe} = 0.412 are shown in Fig. 1. We used the Paterson (1982) calibration to determine the water content from FT-IR absorption using,

$$C_{OH} = \frac{B_i}{150\xi} \int \frac{K(v)}{(3780 - v)} dv \tag{1}$$

where C_{OH} is the molar concentration of hydroxyl ($H/10^6$ Si), B_i is the density factor (4.39×10^4 cm $H/10^6$ Si), ξ is the orientation factor (1/3), and $K(v)$ is the absorption coefficient in cm^{-1} at wavenumber v in cm^{-1} (if the Bell calibration (Bell et al., 2003) is used the water content will be ~3 times larger). The integration was made from 3000 to 3750 cm^{-1}.

The water content of the original sample is less than 8 $H/10^6$ Si (0.0001 wt% H_2O). After the olivine was annealed under the hydrous environment, samples containing different water contents (84–620 ppm wt) were obtained. The water loss during the electrical conductivity measurements of hydrous sample was less than 7% of the initial value.

2.2. Methods of conductivity measurements

Electrical conductivity was measured at P (pressure)=4 GPa at T (temperature) = 873–1273 K for hydrous samples and 873–1473 K for anhydrous samples. The experimental sample assembly is shown in Fig. 2. Pressure was generated by eight cubic tungsten carbide anvils ($26 \times 26 \times 26$ mm^3) with an 18 mm truncated edge length. Pressure calibrations were conducted using the phase transitions of coesite to stishovite (Zhang et al., 1996) (9.5 GPa at
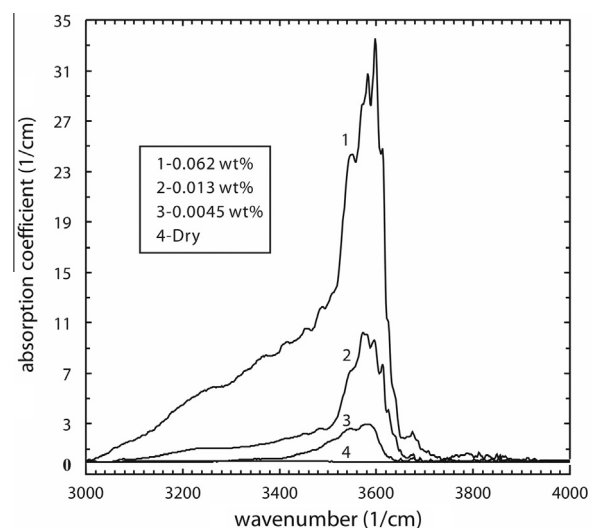
Table 1
Chemical compositions of the starting material of synthetic olivines (numbers in the top column are in wt%).

Oxides	Sample A	Sample B	Sample C
Cr_2O_3	0.01	0.01	0.01
MnO	0.16	0.15	0.14
FeO	19.84	36.03	50.91
NiO	0.03	0.01	0.01
SiO_2	38.73	36.46	32.69
CaO	0.01	0.01	0.01
TiO_2	0.02	0.01	0.01
Al_2O_3	0.01	0.01	0.01
MgO	40.94	28.90	16.25
Pt	0.01	0.01	0.01
Total	99.76	101.60	100.05
Molar percentage			
Forsterite	78.6 ± 0.7	58.8 ± 0.4	36.3 ± 0.3
Fayalite	21.4 ± 0.7	41.2 ± 0.4	63.7 ± 0.3

Fig. 1. The representative FT-IR spectra of synthetic olivine aggregates with X_{Fe} (Fe/(Fe + Mg)) = 0.412 for the wavenumber range of 3000–4000 cm^{-1}.
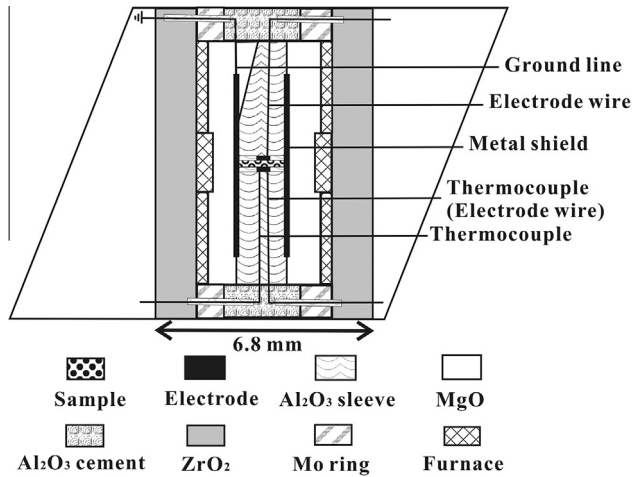
Fig. 2. The experimental setup for electrical conductivity measurements at high pressure and temperature.

1573 K). In order to avoid the influence of adsorbed water on the measurement of electrical conductivity, all sample assembly parts were heated to 1223 K for 12 h prior to each experiment. In order to control the oxygen fugacity of the sample chamber and reduce the leakage currents, a Ni foil shield was placed between a sample and an MgO insulation tube. A disk-shaped sample ($\Phi 1.6 \times 0.4$–0.6 mm) was placed between two parallel Ni electrodes that were surrounded by alumina rings. The temperature was measured by a $W_{5\%}Re$–$W_{26\%}Re$ thermocouple that is attached to another side of Ni electrode (Ni is in direct contact with a sample). The experimental errors of the pressure and temperature were estimated to be no more than 0.5 GPa and 10 K, respectively (absolute error in pressure estimate can be larger but the relative error is ~0.5 GPa or less). The errors in electrical conductivity measurement through the impedance fitting were estimated to be less than 3%.

The pressure was first raised at the rate of ~1.0 GPa/h to a designated pressure. Under a constant pressure condition, temperature was raised at the rate of ~60 K/min to the preset value and the impedance spectroscopy measurements were performed at various temperatures. After the temperature reached to an each value for a constant pressure condition, the ZPlot program of a Solartron-1260 Impedance/Gain-Phase analyzer was run to determine the complex impedance for the frequency range of $f = 10^{-2}$–10^6 Hz for a sinusoidal alternating current of signal voltage of 1.0 V. The impedance semi-circle arc of high frequency branch (10^3–10^6 Hz) was fitted by virtue of an equivalent circuit of the ZView program that was made up of a resistor connected in parallel with a capacitor. From the fitting of the semi-circle to this model, we determined the conductivity of a sample. In most of the runs, the conductivity was determined with decreasing temperature after the peak temperature was reached. However, in a few runs, we determined the conductivity during both heating and cooling. In these cases, we recognized negligible hysteresis suggesting the negligible effect of water (hydrogen) loss. All experimental conditions including water content before and after each experiment, pressure and temperature are summarized in Table 2.

3. Results

The representative impedance spectroscopy results of polycrystalline olivine with the iron content ($X_{Fe} = Fe/(Fe + Mg) = 0.412$, molar ratio) and the water content of ~0.0045 wt% measured at 4 GPa, 873–1273 K are shown in Fig. 3. Results obtained under other conditions are qualitatively similar to those illustrated here.

We observed two circles at high temperatures, whereas only one circle was observed at low temperatures. The presence of two circles in the impedance spectroscopy implies two processes of charge transfer and blocking. The first circle originated at the origin ($Z' = Z'' = 0$) likely corresponds to a parallel combination of resistor and capacitor, and the second circle likely represents the conduction process between sample and electrode (Barkmann and Cemič, 1996; Tyburczy and Roberts, 1990). The presence of a capacitor in the impedance response implies that there are mechanisms to accumulate electric charge in the sample. They include the charge transfer at the sample-electrode interface and the blocking of charge transfer at grain-boundaries.

The electrical conductivities of the samples were calculated using the following equation,

$$\sigma = \frac{L/S}{R} = \frac{L}{SR} \qquad (2)$$

where L is the sample length and S is the cross section area of the electrode. Both L and S are determined before and after each experiment and only small changes in L and S are observed (less than 3%).

The results are shown in Figs. 4–6. Fig. 4 shows the influence of temperature and water content on the hydrous and anhydrous synthetic olivine with the iron content of $X_{Fe} = 0.412$ at 4.0 GPa. Fig. 5 shows the relation between electrical conductivity with the iron content of $X_{Fe} = 0.412$ and water content under conditions of 4 GPa and 873–1273 K. Fig. 6 shows the effect of iron content (X_{Fe}) on the electrical conductivity of anhydrous synthetic olivine aggregates at 4 GPa and 873–1473 K. Fig. 7 shows the effect of chemical composition on the electrical conductivity of dry and a 0.013 wt% water content synthetic olivine 4 GPa.

In both hydrous and anhydrous samples, conductivity increases with FeO content. However, the manner in which conductivity increases with FeO content is different between anhydrous and hydrous samples. For anhydrous samples, the activation enthalpy decreases ~27 kJ/mol from $X_{Fe} = 0.214$ to 0.637, and consequently, the influence of FeO content is large at relatively low temperature but small at relatively high temperatures (the difference in conductivity between $X_{Fe} = 0.214$ and 0.637 is by a factor of ~15 at $T = 873$ K, but the difference is by a factor of ~3 at 1473 K). For hydrous samples, the activation enthalpy (80–88 kJ/mol) is nearly independent of FeO content, and therefore the magnitude of FeO effect is nearly independent of temperature. The difference in conductivity between samples of $X_{Fe} = 0.214$ and 0.637 is by a factor of ~2 at all temperatures.

The observed different effects of FeO content for water-poor (dry) and water-rich (wet) samples suggests that the microscopic mechanisms of electrical conductivity are different between the two, and consequently, we summarize the above results using the following equation,

$$\sigma = \sigma_{o,\text{wet}} \cdot \left(\frac{C_w}{C_{w0}} \right)^r \cdot \exp\left(-\frac{H^*_{\text{wet}}}{RT} \right) + \sigma_{o,\text{dry}} \exp\left(-\frac{H^*_{\text{dry}}}{RT} \right) \qquad (3)$$

where $\sigma_{o,\text{wet(dry)}}$ is the pre-exponential term for wet (dry) mechanism, C_w is water content of the sample, C_{w0} is the reference water content (0.013 wt%), r is a non-dimensional parameter and $H^*_{\text{wet(dry)}}$ is the activation enthalpy for wet (dry) mechanism. We assumed the following functional relationships for these terms

$$\log_{10}\sigma_o = \log_{10}\sigma_{oo} + B \cdot X_{Fe} \qquad (4)$$

and

$$H^* = H^*_o + C \cdot X_{Fe} \qquad (5)$$

where B and C are the parameters that represent the FeO content dependence of pre-exponential term and the activation enthalpy respectively. The parameter r is determined for a sample with $X_{Fe} = 0.412$ ($r = 0.84 \pm 0.12$) and is assumed to be independent

Table 2
Summary of runs.

| Run no.	X_{Fe}	P (GPa)	T (K)	Water content			
				Before experiment		After experiment	
				ppm wt	H/10^6 Si	ppm wt	H/10^6 Si
K1362	0.214	4	873–1273	364	5663	347	5398
K1364	0.214	4	873–1473	<0.45	<7	<0.58	<9
K1359	0.412	4	873–1473	<0.19	<3	<0.39	<6
K1366	0.412	4	873–1273	135	2093	143	2217
K1368	0.412	4	873–1273	612	9523	616	9586
K1376	0.412	4	873–1273	44	689	45	705
K1373	0.637	4	873–1273	84	1311	83	1293
K1375	0.637	4	873–1473	<0.32	<5	<0.51	<8
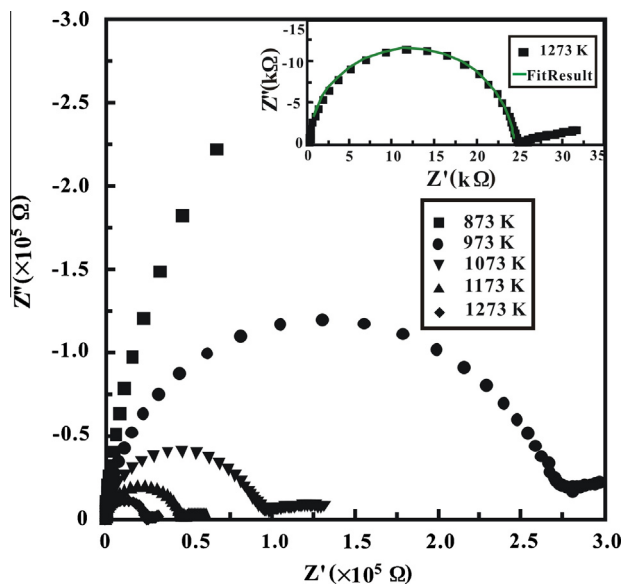
Fig. 3. A Z' vs. Z'' plot of complex impedance of hydrous olivine aggregates with X_{Fe} (Fe/(Fe + Mg)) = 0.412 from 10^{-2} to 10^6 Hz (right to left), obtained under conditions of 4.0 GPa, 873–1273 K and 0.0045 wt% water content. Fit results by equivalent circuit for impedance spectroscopy were also shown. Z' and Z'' are the real and imaginary part of complex impedance respectively.
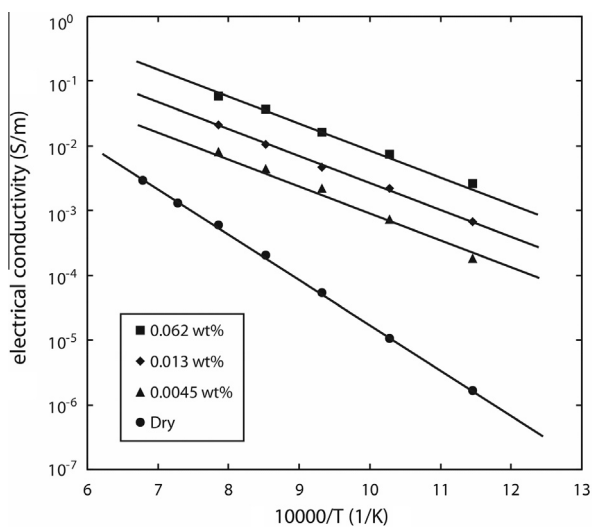

Fig. 4. Electrical conductivity of synthetic olivine with X_{Fe} (=(Fe/(Fe + Mg))) = 0.412 inverse temperature relationship at 4 GPa and 873–1473 K for different water contents.
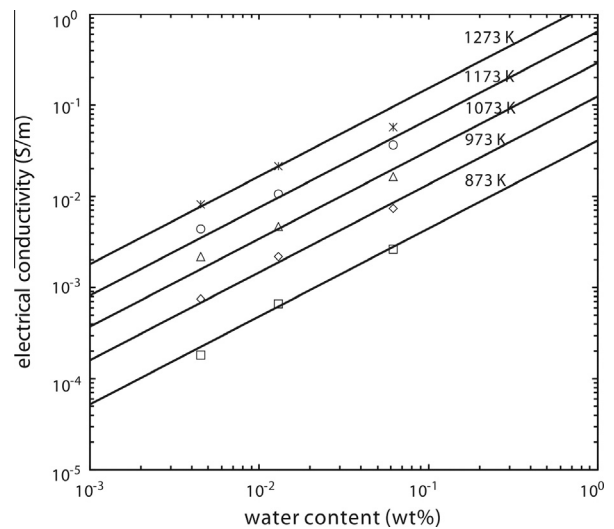

Fig. 5. Electrical conductivity versus water content relation for hydrous olivine aggregates with an X_{Fe} (=(Fe/(Fe + Mg))) = 0.412 under conditions of 4 GPa and 873–1273 K. The fit of the data to a model equation yields $r = 0.84 \pm 0.12$. The numbers along each line represent the temperature in K. Each symbol corresponds to the data for a given temperature (in K).

of X_{Fe}. Other parameters in these equations are summarized in Tables 3 and 4.

4. Discussions

4.1. A comparison to previous studies

Our results on the influence of FeO content on the electrical conductivity of dry olivine are compared to some of the previous studies (Fig. 6) (Cemič et al., 1980; Hirsch et al., 1993; Omura et al., 1989; Wang et al., 2006; Yoshino et al., 2012). The agreement with Hirsch et al. (1993) and Wang et al., 2006) is very good,[1] but there are substantial differences between our results and those by Cemič et al. (1980), Omura et al. (1989) and Yoshino et al. (2012). The results by Cemič et al. (1980), Omura et al. (1989) and Yoshino et al., (2012) show substantially higher conductivity than ours and the sensitivity to FeO content is much higher. All of these studies were made at high pressures, but the water content of samples was not measured by Cemič et al. (1980) and Omura et al. (1989). Yoshino et al. (2012) reported that their ringwoodite sample had a substantial amount of water but the water content of olivine

---

[1] Hirsch et al. (1993) assumed a constant activation energy, while we found that the activation energy changes with FeO content. This difference is due to the fact that Hirsch et al. (1993) used a narrow temperature range and small differences in the activation energy were not detected.
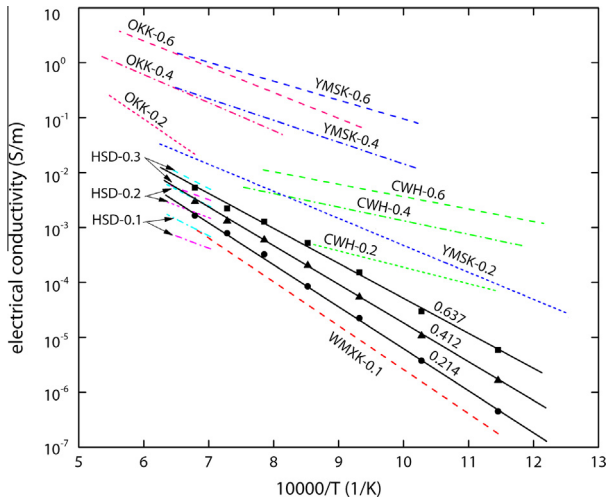
Fig. 6. A comparison of the previous studies on the effect of FeO content (numbers for each data are X_{Fe}) on the electrical conductivity of anhydrous synthetic olivine aggregates. The results from Hirsch et al. (1993) (HSD) are at room pressure, but all others are at $P = 4$ GPa. The black solid lines represent the Arrhenius plot of electrical conductivity of samples in the present study, the cyan and magenta dashed lines (HSD) are from Hirsch et al. (1993) (corresponding to two different parameterizations), the green dashed lines (CWH) are from Cemič et al. (1980), the pink dashed lines (OKK) are from Omura et al. (1989), the blue dashed lines are from Yoshino et al. (2012) and the red dashed one (WMXK) is from Wang et al. (2006)'s dry sample with FeO content of $X_{Fe} = 0.1$, respectively. Hirsch et al. (1993) measured the conductivity only for $X_{Fe} = 0.09$–0.34, so the results corresponding to $X_{Fe} = 0.1$, 0.2 and 0.3 are shown. (For interpretation of color in Fig. 6, the reader is referred to the web version of this article.)
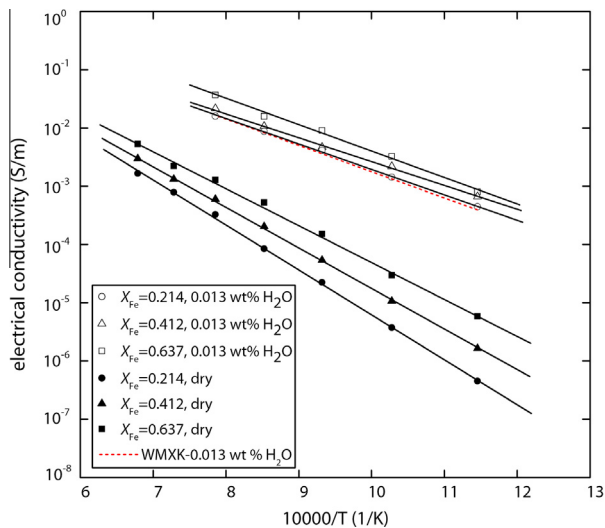

Fig. 7. The effect of FeO content on the electrical conductivity of anhydrous and hydrous synthetic olivine aggregates at 4 GPa, 873–1473 K and the water content of 0.013 wt%. For hydrous samples with different iron content were normalized to $C_W = 0.013$ wt% by using $\sigma \propto C_W^r$ with $r = 0.84 \pm 0.12$ (C_W: water content). The actual values of r for different compositions could be different. A variation in r by ±0.2 would lead to an uncertainty in estimated conductivity of ~20%. A comparison with Wang et al. (2006)'s hydrous result was conducted for the samples of $X_{Fe} = 0.1$ and the same water content.

samples was not reported. Therefore a part of the difference could be due to water in case of Cemič et al. (1980), Omura et al. (1989) and Yoshino et al. (2012). In addition, in Cemič et al. (1980) and Omura et al., (1989), electrical conductivity was measured only at one frequency. This can introduce systematic errors in the calculated conductivity (e.g., (Karato and Dai, 2009; Karato and Wang, 2013)).

The most puzzling observation is the large difference between our results and those by Yoshino et al. (2012) because in both

studies, essentially the same technique (impedance spectroscopy) was used at similar pressures and temperatures. The reason for this disagreement is not known but we note that our results are in very good agreement with the room pressure results by Hirsch et al. (1993). Room pressure experiments on electrical conductivity are much more free from any technical problems, and because the pressure effects on conductivity are very small (e.g., (Xu et al., 2000; Dai and Karato, 2014a)), we consider that a good agreement of our results with Hirsch et al. (1993) support the robustness of our experimental results. However, it is impossible to interpret Yoshino et al. (2012)'s results because the water content of their nominally "dry" olivine samples is unknown. It is essential that the water content of the samples is measured both before and after each conductivity measurement to obtain reliable experimental data (Karato and Wang, 2013).

The influence of FeO on hydrogen-assisted electrical conductivity of olivine was not studied before, but a comparison to Wang et al. (2006) shows an excellent agreement (Fig. 7). Our results show that hydrogen-assisted conductivity in olivine increases with FeO content, but the magnitude of the effect of FeO is only modest. Interestingly, the activation energy of hydrogen-assisted conduction is nearly independent of FeO content as opposed to the activation energy for anhydrous olivine ("polaron" conduction). This implies that the mobility of proton in olivine is not much affected by the FeO content. One possible explanation is to consider a model that the barrier for proton migration is the strain energy associated with the proton-related defect (Dai and Karato, 2014a). In such a case, the strain energy is largely controlled by the weak H—O bonds and is slightly affected by the strain energy in other regions. Dai and Karato (2014a) showed that such a model could explain the observed negative activation volume. Finally, a slight increase in hydrogen-assisted conductivity with FeO content might be caused by the increase in mobile hydrogen ("free" hydrogen) with FeO content. This is possible because the concentration of free proton depends on the ionization energy of $(2H)_M^\times$ (two proton trapped at M-site vacancy) that becomes smaller with a larger FeO content because of the increase in the static dielectric constant (Karato, 1981).

In contrast to the weak effect of FeO on hydrogen-assisted conduction in olivine, the influence of hydrogen content on hydrous olivine is large. Our results are similar to most of the previous studies (e.g., (Poe et al., 2010; Wang et al., 2006; Yoshino et al., 2009)) to the extent that all of these studies show a substantial effect of water (hydrogen) to enhance electrical conductivity (our results agree very well with those by Wang et al. (2006), see Fig. 7). However, the water content exponent determined for $X_{Fe} = 0.412$ ($r = 0.84 \pm 0.12$) samples was slightly higher than the value reported by Wang et al. (2006) for San Carlos olivine ($r = 0.62 \pm 0.15$). The difference might be due to the different degree of contribution of two different mechanisms of conduction (Dai and Karato, 2014b; Karato, 2013b) for samples with different FeO content. There have been debates on how water (hydrogen) enhances electrical conductivity in minerals (e.g., (Karato and Wang, 2013; Yoshino and Katsura, 2013)). This issue on olivine has been discussed in detail based on our new results on the pressure effect (Dai and Karato, 2014a), the oxygen fugacity effect (Dai and Karato, 2014c), and the temperature effects (Dai and Karato, 2014b; Karato, 2013b). Therefore we will not repeat these discussions here. Briefly, all of these studies support a hybrid model of hydrogen-assisted conduction that also explains the cause of apparent "discrepancy".

4.2. Potential applications to planetary interiors

The present results have potential applications for the interpretation of inferred electrical conductivity in other terrestrial bodies

Table 3
Composition of the samples and the corresponding pre-exponential term and activation enthalpy.

Samples	X_{Fe} (Fe/(Fe + Mg), molar ratio)	C_w (wt%)	Log_{10} σ_o(S/m)	H^*(kJ mol^{-1})
Wet (all data)	0.214	0.035	2.0 ± 0.1	83 ± 2
	0.412	0.062	2.13 ± 0.3	80 ± 7[§]
	0.412	0.013	1.56 ± 0.2	80 ± 7[§]
	0.412	0.0045	1.14 ± 0.2	80 ± 7[§]
	0.637	0.0084	1.91 ± 0.3	88 ± 4
Dry (all data)	0.214	-	2.5 ± 0.2	148 ± 3
	0.412	-	2.3 ± 0.1	136 ± 6
	0.637	-	2.0 ± 0.3	121 ± 4

[§] Activation energy is assumed to be independent of water content.

Table 4
Parameter values of pre-exponential factor σ_o and activation enthalpy H^* for the electrical conductivity of anhydrous and hydrous synthetic polycrystalline olivine with different chemical compositions. The relation $\sigma = \sigma_o(X_{Fe}) \cdot \left(\frac{C_w}{C_{w0}}\right)^r \cdot \exp\left[-\frac{H^*(X_{Fe})}{RT}\right]$ is assumed with $\log_{10}\sigma_0 = \log_{10}\sigma_{00} + B \cdot X_{Fe}$ and $H^* = H_o^* + C \cdot X_{Fe}$ (X_{Fe} is the molar ratio, Fe/(Fe + Mg)) with $r = 0$ for dry condition and 0.013 wt% ($r = 0.84 \pm 0.12$). Errors are one standardized deviation, and include the contribution of errors in individual measurements (errors in water content, temperature and electrical conductivity).

$ALog_{10}$ σ_o (S/m)	H^* (kJ/mol)
Anhydrous	
Log_{10} σ_{00} = 2.77 (±0.38)	H_o^* = 162 (±9)
B = −1.19 (±0.09)	C = −63 (±4)
Hydrous	
Log_{10} σ_{00} = −1.42 (±0.26)	H_o^* = 82 (±10)
B = 1.08 (±0.12)	C = 7.2 (±0.3)

such as Mars. Studies on Martian meteorites suggest some water in Martian mantle (Dreibus and Wänke, 1987; McSween, 1985; McSween and Harvey, 1993). However, the interpretation of these samples is controversial because these samples came to near surface after complicated processes. Electromagnetic induction observations would provide constraints on the electrical conductivity of a planet such as Mars (Verhoeven et al., 2005).

These results can provide useful constraints on the water content in a planet. However, each planet has different major element chemical compositions including FeO content, and the influence of FeO content needs to be evaluated before such a study can be made. In this context, the observed small FeO dependence of hydrogen-assisted conduction in olivine implies that when one wants to estimate hydrogen content from geophysically inferred conductivity in a planet, the influence of FeO content is minor and can be ignored to a good approximation. For instance, in Mars, FeO content is about $X_{Fe} = 0.25$ compared to ~0.10 for Earth. Between these compositions, hydrogen-assisted conductivity changes only by ~50% (for the same hydrogen content). The hydrogen content we wish to determine is its order of magnitude. Therefore the possible influence of FeO is so small that one can safely ignore the influence of FeO. Similarly, Karato (2011) showed that the influence of mineralogy such as olivine to orthopyroxene ratio has only modest influence on electrical conductivity.

In addition to FeO content, other factors could affect the interpretation of conductivity data in other planets (satellites). For instance, there are some suggestions for low oxygen fugacity, fO_2, in the lunar interior although deep interior might have higher fO_2 (e.g., (Wieczorek et al., 2006)). The influence of fO_2 on hydrogen-related conduction in olivine was determined by Dai and Karato (2014c) and therefore the influence of fO_2 can be corrected if fO_2 in these planets were known. However the magnitude of correction is not very large (a change in fO_2 by three orders of magnitude will change the electrical conductivity by a factor of ~2)

compared to the uncertainties in other factors (e.g., temperature, inferred magnitude of conductivity). Similarly, there is some evidence as to sulfur-rich Martian interior (e.g., (Gaillard et al., 2013; Gaillard and Scaillet, 2009)). In such a case, the influence of sulfide melt would need to be considered although the influence of partial melt is complicated by the strong role of gravity-induced compaction (Karato, 2014).

In summary, geophysical observations (via the measurements of electromagnetic induction, e.g., (Sonett, 1982; Verhoeven et al., 2005)) provide promising data to infer the hydrogen (water) content in terrestrial planet such as Mars. The present results provide one of the key experimental data sets in doing such an endeavor. However, the trade-off between water content and other parameters such as temperature needs to be examined, say by a combination with other observations such as tidal dissipation (e.g., (Karato, 2013a)).

References

Barkmann, T., Cemič, L., 1996. Impedance spectroscopy and defect chemistry of fayalite. Phys. Chem. Miner. 23, 186–192.

Bell, D.R., Rossman, G.R., Maldener, J., Endisch, D., Rauch, F., 2003. Hydroxide in olivine: a quantitative determination of the absolute amount and calibration of the IR spectrum. J. Geophys. Res. 108. http://dx.doi.org/10.1029/2001JB000679.

Bertka, C.M., Fei, Y., 1997. Mineralogy of the Martian interior up to the core-mantle boundary. J. Geophys. Res. 107, 5251–5264.

Cemič, L., Will, G., Hinze, E., 1980. Electrical conductivity measurements on olivines Mg_2SiO_4-Fe_2SiO_4 under defined thermodynamic conditions. Phys. Chem. Miner. 6, 95–107.

Dai, L., Karato, S., 2009. Electrical conductivity of wadsleyite under high pressures and temperatures. Earth Planet. Sci. Lett. 287, 277–283.

Dai, L., Karato, S., 2014a. The effect of pressure on hydrogen-assisted electrical conductivity of olivine. Phys. Earth Planet. Inter. 232, 51–56.

Dai, L., Karato, S., 2014b. High and highly anisotropic electrical conductivity of the asthenosphere caused by hydrogen diffusion in olivine. Earth Planet. Sci. Lett. 408, 79–86.

Dai, L., Karato, S., 2014c. Influence of oxygen fugacity on the electrical conductivity of olivine under hydrous conditions: implications for the mechanism of conduction. Phys. Earth Planet. Inter. 232, 57–60.

Dreibus, G., Wänke, H., 1987. Volatiles on earth and mars: a comparison. Icarus 71, 225–240.

Elkins-Tanton, L., Grove, T.L., 2011. Water (hydrogen) in the lunar mantle: results from petrology and magma ocean modeling. Earth Planet. Sci. Lett. 307, 173–179.

Gaillard, F., Michalski, J., Berger, G., McLennan, S.M., Scaillet, B., 2013. Geochemical reservoirs and timing of sulfur cycling on Mars. Space Sci. Rev. 174, 251–300.

Gaillard, F., Scaillet, B., 2009. The sulfur content of volcanic gases on Mars. Earth Planet. Sci. Lett. 279, 34–43.

Grott, M., Baratoux, D., Hauber, E., Breuer, D., Karato, S., Knapmeyer, M., Ruff, S., Sohl, F., Sautter, V., Gasnault, O., McLennan, S.M., Morschhauser, A., 2013. Long-term evolution of the crust-mantle system of Mars. Space Sci. Rev. 174, 49–111.

Hirsch, L.M., Shankland, T.J., Duba, A., 1993. Electrical conduction and polaron mobility in Fe-bearing olivine. Geophys. J. Int. 114, 36–44.

Karato, S., 1981. Rheology of the lower mantle. Phys. Earth Planet. Inter. 24, 1–14.

Karato, S., 1990. The role of hydrogen in the electrical conductivity of the upper mantle. Nature 347, 272–273.

Karato, S., 2011. Water distribution across the mantle transition zone and its implications for global material circulation. Earth Planet. Sci. Lett. 301, 413–423.

Karato, S., 2013a. Geophysical constraints on the water content of the lunar mantle and its implications for the origin of the Moon. Earth Planet. Sci. Lett. 384, 144–153.

Karato, S., 2013b. Theory of isotope diffusion in a material with multiple-species and its implications for hydrogen-enhanced electrical conductivity in olivine. Phys. Earth Planet. Inter. 219, 49–54.

Karato, S., 2014. Does partial melting explain geophysical anomalies? Phys. Earth Planet. Inter. 228, 300–306.

Karato, S., Dai, L., 2009. Comments on "Electrical conductivity of wadsleyite as a function of temperature and water content" by Manthilake et al.. Phys. Earth Planet. Inter. 174, 19–21.

Karato, S., Wang, D., 2013. Electrical conductivity of minerals and rocks. In: Karato, S. (Ed.), Physics and Chemistry of the Deep Earth. Wiley-Blackwell, New York, pp. 145–182.

Khan, A., Connolly, J.A.D., Maclennan, J., Mosegaard, K., 2007. Joint inversion of seismic and gravity data for lunar composition and thermal state. Geophys. J. Int. 168, 243–258.

McSween Jr., H.Y., 1985. SNC meteorites: clues to Martian petrologic evolution? Rev. Geophys. 23, 391–416.

McSween, H.Y.J., Harvey, R.P., 1993. Outgassed water on Mars: constraints from melt inclusions in SNC meteorites. Science 259, 1890–1892.

Nittler, L.R., Starr, R.D., Weider, S.Z., McCoy, T.J., Boynton, W.V., Ebel, D.S., Ernst, C.M., Evans, L.G., Goldsten, J.O., Hamara, D.K., Lawrence, D.J., McNutt Jr., R.L., Schlemm II., C.E., Solomon, S.C., Sprague, A.L., 2011. The major-element composition of Mercury's surface from MESSENGER X-ray spectroscopy. Science 333, 1847–1850.

Omura, K., Kurita, K., Kumazawa, M., 1989. Experimental study of pressure dependence of electrical conductivity of olivine at high temperatures. Phys. Earth Planet. Inter. 57, 291–303.

Paterson, M.S., 1982. The determination of hydroxyl by infrared absorption in quartz, silicate glass and similar materials. Bull. Mineral. 105, 20–29.

Poe, B., Romano, C., Nestola, F., Smyth, J.R., 2010. Electrical conductivity anisotropy of dry and hydrous olivine at 8 GPa. Phys. Earth Planet. Inter. 181, 103–111.

Sonett, C.P., 1982. Electromagnetic induction in the Moon. Rev. Geophys. Space Phys. 20, 411–455.

Tyburczy, J.A., Roberts, J.J., 1990. Low frequency electrical response of polycrystalline olivine compacts: grain boundary transport. Geophys. Res. Lett. 17, 1985–1988.

Vacher, P., Verhoeven, O., 2007. Modelling the electrical conductivity of iron-rich minerals for planetary applications. Planet. Space Sci. 55, 455–466.

Verhoeven, O., Rivoldini, A., Vacher, P., Mocquet, A., Choblet, G., Menvielle, M., Dehant, V., van Hoolst, T., Sleewaegen, J., Barriot, J.-P., Longnonné, P., 2005. Interior structure of terrestrial planets: modeling Mars' mantle and its electromagnetic, geodetic, and seismic properties. J. Geophys. Res. 110. http://dx.doi.org/10.1029/2004JE002271.

Wang, D., Mookherjee, M., Xu, Y., Karato, S., 2006. The effect of water on the electrical conductivity in olivine. Nature 443, 977–980.

Wieczorek, M.A., Jolliff, B.L., Khan, A., Pritchard, M.E., Weiss, B.P., Williams, J.G., Hood, L.L., Righter, K., Neal, C.R., Shearer, C.K., McCallum, I.S., Tomkins, S., Hawke, B.R., Peterson, C., Gillis, J.J., Bussey, B., 2006. The composition and structure of the lunar interior. Rev. Mineral. Geochem. 60, 221–364.

Xu, Y., Shankland, T.J., Duba, A.G., 2000. Pressure effect on electrical conductivity of mantle olivine. Phys. Earth Planet. Inter. 118, 149–161.

Yoshino, T., 2010. Laboratory electrical conductivity measurement of mantle minerals. Surv. Geophys. 31, 163–206.

Yoshino, T., Katsura, T., 2013. Electrical conductivity of mantle minerals: role of water in conductivity anomalies. Annu. Rev. Earth Planet. Sci. 41, 605–628.

Yoshino, T., Matsuzaki, T., Shatskiy, A., Katsura, T., 2009. The effect of water on the electrical conductivity of olivine aggregates and its implications for the electrical structure of the upper mantle. Earth Planet. Sci. Lett. 288, 291–300.

Yoshino, T., Matsuzaki, T., Yamashita, S., Katsura, T., 2006. Hydrous olivine unable to account for conductivity anomaly at the top of the asthenosphere. Nature 443, 974–976.

Yoshino, T., Shimojuku, A., Shan, S., Guo, X., Yamazaki, D., Ito, E., Higo, Y., Funakoshi, K., 2012. Effect of temperature, pressure and iron content on the electrical conductivity of olivine and its high-pressure polymorphs. J. Geophys. Res. 117. http://dx.doi.org/10.1029/2011JB008774.

Zhang, J., Li, B., Utsumi, W., Liebermann, R.C., 1996. In situ X-ray observations of the coesite-stishovite transition: reversed phase boundary and kinetics. Phys. Chem. Miner. 23, 1–10.

Zhao, Y.-H., Ginsberg, S.B., Kohlstedt, D.L., 2004. Solubility of hydrogen in olivine: dependence on temperature and iron content. Contrib. Miner. Petrol. 147, 155–161.